



Article

Effectiveness Trade-Off Between Green Spaces and Built-Up Land: Evaluating Trade-Off Efficiency and Its Drivers in an Expanding City

Xinyu Dong ^{1,2,3,*}, Yanmei Ye ³, Tao Zhou ^{2,4}, Dagmar Haase ^{1,2}  and Angela Lausch ^{1,2,5,6} 

¹ Department of Computational Landscape Ecology, Helmholtz Centre for Environmental Research–UFZ, 04318 Leipzig, Germany; dagmar.haase@geo.hu-berlin.de (D.H.); angela.lausch@ufz.de (A.L.)

² Landscape Ecology Lab, Geography Department, Humboldt-Universität zu Berlin, 10099 Berlin, Germany; tao.zhou@ldu.edu.cn

³ Department of Land Management, Zhejiang University, Hangzhou 310058, China; yeyanmei@zju.edu.cn

⁴ School of Resources and Environmental Engineering, Ludong University, Yantai 264025, China

⁵ Department of Physical Geography and Geoecology, Martin Luther University Halle-Wittenberg, 06120 Halle, Germany

⁶ Department of Architecture, Facility Management and Geoinformation, Institute for Geo-Information and Land Surveying, Anhalt University of Applied Sciences, 06846 Dessau, Germany

* Correspondence: xinyu.dong@ufz.de

Abstract: Urban expansion encroaches on green spaces and weakens ecosystem services, potentially leading to a trade-off between ecological conditions and socio-economic growth. Effectively coordinating the two elements is essential for achieving sustainable development goals at the urban scale. However, few studies have measured urban–ecological linkage in terms of trade-off. In this study, we propose a framework by linking the degraded ecological conditions and urban land use efficiency from a return on investment perspective. Taking a rapidly expanding city as a case study, we comprehensively quantified urban–ecological conditions in four aspects: urban heat island, flood regulating service, habitat quality, and carbon sequestration. These conditions were assessed on 1 km² grids, along with urban land use efficiency at the same spatial scale. We employed the slack-based measure model to evaluate trade-off efficiency and applied the geo-detector method to identify its driving factors. Our findings reveal that while urban–ecological conditions in Zhengzhou’s periphery degraded over the past two decades, the inner city showed improvement in urban heat island and carbon sequestration. Trade-off efficiency exhibited an overall upward trend during 2000–2020, despite initial declines in some inner city areas. Interaction detection demonstrates significant synergistic effects between pairs of drivers, such as the Normalized Difference Vegetation Index and building height, and the number of patches of green spaces and the patch cohesion index of built-up land, with q -values of 0.298 and 0.137, respectively. In light of the spatiotemporal trend of trade-off efficiency and its drivers, we propose adaptive management strategies. The framework could serve as guidance to assist decision-makers and urban planners in monitoring urban–ecological conditions in the context of urban expansion.

Keywords: urban land use efficiency; ecological condition; SBM model; trade-off efficiency; urban–ecological linkage



Academic Editor: Yuji Murayama

Received: 17 October 2024

Revised: 6 January 2025

Accepted: 7 January 2025

Published: 9 January 2025

Citation: Dong, X.; Ye, Y.; Zhou, T.; Haase, D.; Lausch, A. Effectiveness Trade-Off Between Green Spaces and Built-Up Land: Evaluating Trade-Off Efficiency and Its Drivers in an Expanding City. *Remote Sens.* **2025**, *17*, 212. <https://doi.org/10.3390/rs17020212>

Copyright: © 2025 by the authors.

Licensee MDPI, Basel, Switzerland.

This article is an open access article distributed under the terms and

conditions of the Creative Commons Attribution (CC BY) license

(<https://creativecommons.org/licenses/by/4.0/>).

1. Introduction

Urban expansion is a rapidly evolving global concern that has gained significant attention. Recent data reveal that the urbanization rate in many developed countries has

exceeded 85% and is still increasing [1]. China is also experiencing rapid urban growth, with the urbanization rate rising from 50% to 64% over the past decade [2]. Although urbanization drives economic growth and contributes to social development, this anthropogenic process usually encroaches on green spaces, which provide multifarious ecosystem services that are essential for maintaining regional ecological conditions [3]. For example, Peng et al. [4] demonstrated that the surface urban heat island range and intensity in urban expansion areas has significantly increased by 71% and 81% in 31 major Chinese cities, respectively. Yue et al. [5] reported that the habitat quality has shown a marked decline in about 30% of the Chinese border areas since 1985 due to built-up land expansion.

From a global perspective, urban–ecological trade-offs are widely evident. For example, Kabisch and Haase [6] demonstrated that numerous European cities experienced significant ecological deterioration due to commercialization, real estate development, and population growth during urbanization. In Africa, urban expansion coupled with overexploitation of natural resources has resulted in extensive losses of farmland, forests, and natural areas. Environmental conditions within these rapidly growing urban areas have severely deteriorated. Climate change has further exacerbated these issues, with cities like Lagos, Addis Ababa, and major South African urban centers experiencing intensified flooding and urban heat island effects [7].

In response to the ecological pressure, cities worldwide have implemented various measures such as green infrastructure development, urban forest restoration, and sustainable land use policies to mitigate urban–ecological degradation and enhance ecosystem services [8,9]. The Chinese government has also adjusted its development philosophy to ecological civilization since 2013, committing to achieve sustainable developments [10]. Several greening projects and land use policies, such as intensive land use and ecological redline policies, have been proposed to restrict the extensive expansion of built-up land and maintain a balance between urban development and ecological conditions [11–13]. These measures have measurably improved the vegetation cover and ecological conditions in many Chinese cities [14]. However, despite this progress, Chinese cities are continuing to expand and built-up areas are projected to increase by 48% by 2050 [15]. It is foreseeable that the conflict between urban expansion and ecological conditions will persist for a long time, highlighting the significance of monitoring urban–ecological dynamics, which has also attracted growing attention from urban planners, policymakers, and the academic community [16].

Several studies tend to explore the urban–ecological linkage by quantitatively explaining the adverse impacts of urban growth on urban–ecological conditions [17–20]. Except for the explanatory approaches, different approaches have been developed to examine this relationship. For instance, the coupling coordination degree model is widely used to assess the urban–ecological relationship [21]. However, the model assumes an optimal state where both urbanization and ecological conditions reach their maximum levels simultaneously. The Environmental Kuznets Curve, another frequently applied theory, suggests that ecological conditions may initially deteriorate but eventually improve as development reaches a certain threshold [22]. In addition, studies prove a negative correlation between ecological conditions with urban development. For instance, some development-related indicators, including public services, urban population, GDP, etc., are negatively correlated with eco-environmental elements [23–25]. Given the negative relationship, some studies try to measure the urban–ecological linkage from a trade-off perspective, and even treat the degraded ecological conditions as an opportunity cost of urban development [26,27].

However, existing studies on urban–ecological relationships have several limitations. For instance, many evaluations typically focus on single ecological issues such as habitat degradation, urban heat island, or flood risk, lacking a comprehensive perspective [28–30].

Although a number of studies attempt to synthetically capture the degraded ecological conditions arising from urban expansion, the employed indicators are vague: specifically, the volume of discharged urban waste, amounts of renewable energy usage and water resources per capita, albeit not directly associated with the ecological conditions, are often used as evaluation metrics by combining with different weights [31–33]. In addition, studies tend to be carried out at the county level or at larger scales using statistical data, making it challenging to support regional decision-making in urban planning [34,35].

Urban expansion may lead to extensive land use, especially when not properly planned. This low-density or disorganized land development may encroach on green spaces without fully realizing its economic and social potential [36,37]. In contrast, different green spaces provide varying levels of ecosystem services owing to factors like location, vegetation type, and landscape pattern [38,39]. Given the limited land resources, urban expansion creates a potential trade-off between socio-economic output and ecological opportunity cost, and the trade-off efficiency can be further determined by the effectiveness of replaced green spaces and developed built-up land. While the trade-off relationship has been widely corroborated in studies involving urban–ecological interaction [23,25], there has been little research on measuring the urban–ecological linkage in terms of the effectiveness trade-off between green space and built-up land.

Consequently, to address these research gaps, this study aims to propose a trade-off-based evaluation framework that links the effectiveness of green spaces and built-up land from a return on investment. Using a rapidly developing Chinese city of Zhengzhou as a case study, the framework quantifies the urban–ecological conditions in four aspects to reflect the effectiveness of green spaces and applies urban land use efficiency to indicate the effectiveness of built-up land. From a return on investment perspective, we adopt the slack-based measure model to evaluate the trade-off efficiency by considering the degraded ecological conditions as input and treating urban land use efficiency as output. Therefore, trade-off efficiency is a measure that evaluates the cost effectiveness between urban development and its impacts on ecological conditions. A desirable trade-off efficiency can be achieved when using less ecological opportunity costs to yield higher urban development return. Furthermore, the geo-detector method is employed to identify which factors significantly influence the spatial variations in trade-off efficiency.

2. Methods and Materials

2.1. Study Area

Located in the heart of China, Zhengzhou is a bustling metropolis known for its rapid growth and large population as the capital of Henan province. The city has a moderate continental monsoon climate, marked by four distinct seasons and an average yearly rainfall of roughly 650 mm. During the peak of summer, air temperatures can soar above 35 °C. Over the past two decades (2000–2020), the city’s population has doubled from about 6 million, reaching a total of 12.6 million. This has led to an increase in the urbanization rate to 79.1% and a rapid expansion of the built-up area.

The boundary and location of the study area are depicted in Figure 1. According to Zhengzhou Territorial Spatial Planning (2020–2035), the expansion of the main urban area is primarily restricted within the city’s outer ring road. Since this study mainly focuses on urban–ecological linkage, we defined this boundary as the study area. Additionally, in most Chinese cities, urbanization typically decreases along with the urban–rural gradient. The area within the inner ring road can be regarded as the inner city, with development intensity gradually tapering off from this inner boundary outside.

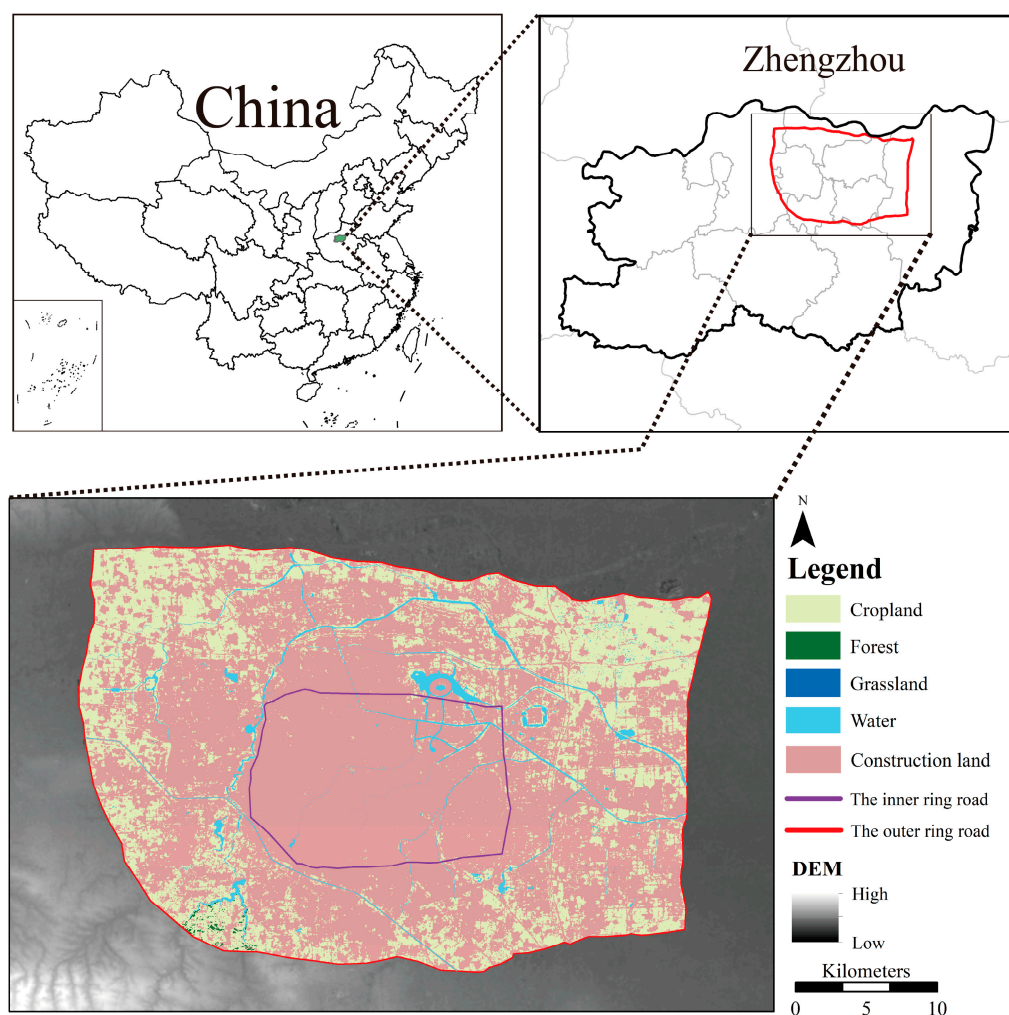


Figure 1. Location and boundary of the study area.

2.2. Methodology

Green spaces provide a variety of ecosystem services, which enhance surrounding ecological conditions through ecosystem processes and flows [40,41]. However, these benefits are often weakened when the green spaces are converted to impervious built-up land during urban sprawls [42]. However, built-up land is essential for providing space for human activities such as living and production, and its expansion is usually related to socio-economic development [43,44]. Therefore, urban expansion may cause a trade-off between the two elements [45]. However, during urban expansion, the effectiveness of the replaced green spaces and the developed built-up land differ, resulting in variations in this trade-off, and the urban–ecological linkage can thus be evaluated through the trade-off efficiency (ToE). Among the ecosystem services provided by green spaces, regulating and supporting services have the most significant impact on ecological conditions and are particularly sensitive in the context of urban expansion [46,47]. Therefore, we identified the urban–ecological conditions across four dimensions to capture the effectiveness of green spaces, including the urban heat island (UHI), flood regulating services (FRSs), habitat quality (HQ), and carbon sequestration (CS). These aspects are widely recognized and commonly used in studies involving urban ecosystems [48,49]. As opposed to urban–ecological conditions, ULUE is a dimensionless variable and is widely used as a proxy for the effectiveness of built-up land [50,51].

The methodological framework for this evaluation is depicted in Figure 2. We first quantified the urban–ecological conditions in the four aspects for three periods (2000,

2010 and 2020) on 1 km² grids using remote sensing retrieval, hydrological models and spatial quantitative models. The ULUE was also calculated at the same resolution by fusing geospatial data for unitary comparison with ecological conditions. The slack-based measure (SBM) model was introduced to evaluate the ToE between the effectiveness of green spaces and built-up land with the four degraded ecological conditions as the input variables, while the ULUE was the output parameter. Then, this study used a geo-detector to analyze the drivers affecting the ToE. We finally proposed adaptive management strategies in light of the spatiotemporal trend of ToE and its drivers. It should be noted that this study excludes water bodies. We retrieved the normalized difference water index from Landsat imageries and extracted the water bodies for the three periods. All spatial data falling onto the water bodies were defined as void. The component described in Figure 2 will be elaborated in the following sections.

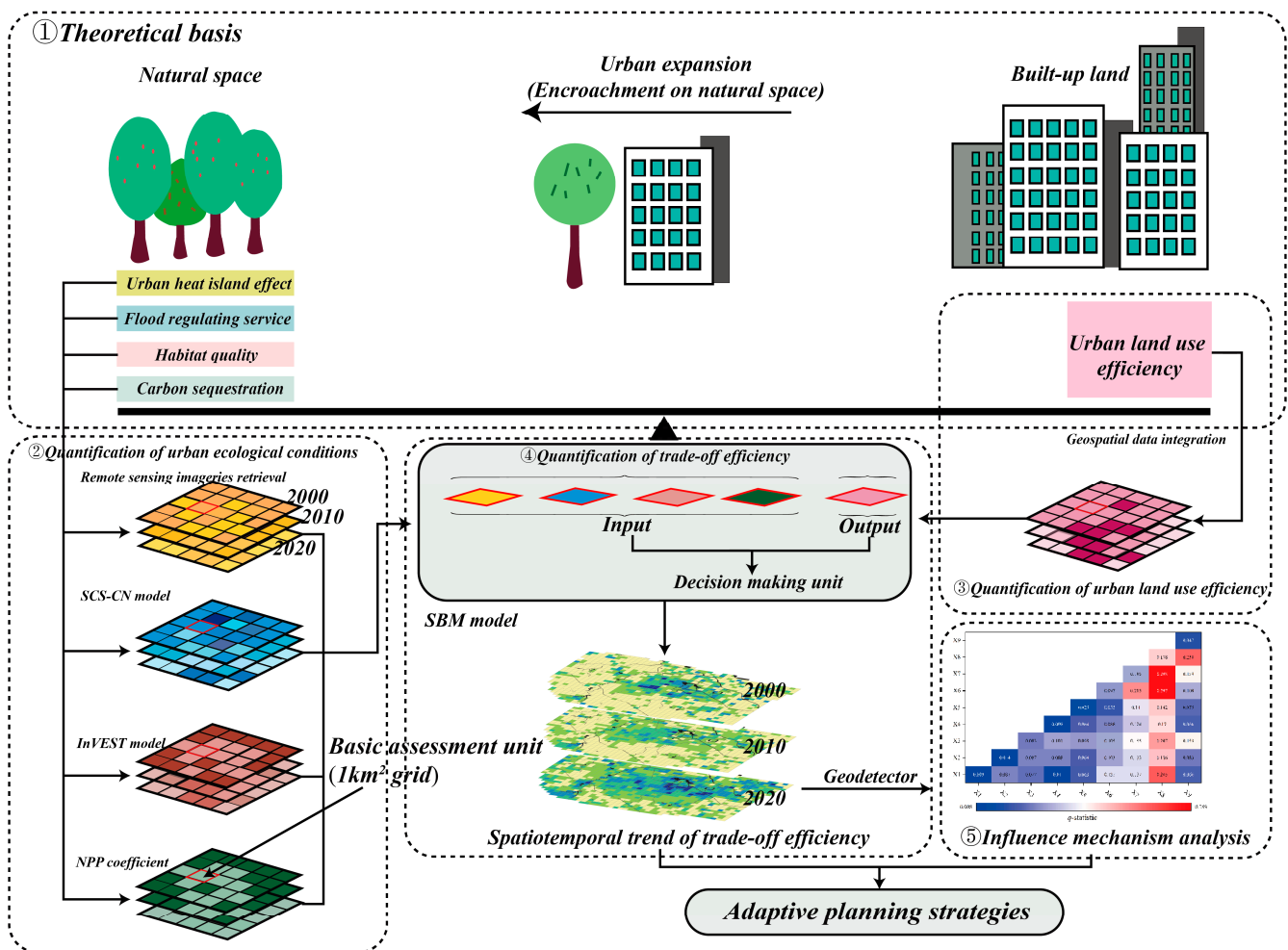


Figure 2. Methodological framework of the study.

2.3. Quantification of Urban–Ecological Conditions

2.3.1. Urban Heat Island

Urban expansion encroaches green spaces and disturbs its landscape pattern, weakening cooling services [52]. We quantified the ecological opportunity cost using the widely adopted urban–rural dichotomy method [53], as described in Equation (1).

$$UHI_i = LST_i - LST_{background} \tag{1}$$

where UHI_i is the urban heat island on the i th assessment unit; LST_i is the average land surface temperature on the i th assessment unit; and $LST_{background}$ is the background temperature.

To characterize the land surface temperature, we obtained all available Landsat Collection 2 level-2 products for the three periods through the Google Earth Engine. We implemented a quality assessment-based cloud masking protocol exclusively within the study area's boundaries to maximize image availability. First, we conducted a cloud-masking function to detect and remove high-confidence clouds and their shadows by examining the cloud (Bit 3), cloud confidence (Bit 4), and cloud shadow (Bit 5) information. Then, using GEE's `reduceRegion` method, we computed the ratio of cloud pixels to total pixels within the study area, selecting images where this ratio did not exceed 5%. For each qualified image, we derived LST values by applying the multiplicative scale factor and offset as specified in the USGS guidelines [54]. We used a maximum value composite from the LST time series to represent the most severe urban heat conditions.

The background temperature is a key factor for this method and was extracted through the following steps [55]: (1) we used a $1\text{ km} \times 1\text{ km}$ moving window method to count the proportion of built-up land based on land use data and generated the built-up intensity map; (2) using 50% built-up area as a threshold, contiguous areas with built-up land over 50% were merged to form the urban core area; (3) the average land surface temperature in the equal-area surroundings of the urban core area, excluding water bodies, their 300 m buffers, and areas with $\pm 50\text{ m}$ of average topographic elevations, was used to extract the background temperature.

2.3.2. Flood Regulating Service

The growth of built-up land usually alters the local natural hydrological cycle, undermining the regional FRS, which may generate extra runoff during rainfall events and trigger flooding risk [56]. We employed the SCS-CN model to quantify the spatiotemporal change in FRS for the trade-off evaluation. This is an empirical hydrological model used for the spatial quantification of runoff generated during precipitation events. However, the model neglects the impact of topographic factors on hydrological processes. For the purpose of more accurate assessments, we adopted Huang's slope modification in the model, which considers the impact of slope on runoff infiltration by modifying the CN value [57]. The higher the runoff depth under a specific rainfall event, the worse the FRS. The runoff depth by this modified model can be quantified by Equations (2)–(5).

$$runoff = \begin{cases} \frac{(P-I_a)^2}{P-I_a+S}, & P \geq I_a \\ 0, & P \leq I_a \end{cases} \quad (2)$$

$$I_a = \lambda \times S \quad (3)$$

$$CN_s = \frac{322.79 + 15.63slope}{slope + 323.52} CN \quad (4)$$

$$S = 25400/CN_s - 254 \quad (5)$$

where $runoff$ is the generated runoff quantity during the precipitation event; P is the rainfall event, which is set to 20-year return period rainfall in accordance with the Zhengzhou City flood control standards; I_a is the initial loss due to depression storage; λ is the initial loss coefficient, which is 0.2 according to the United States Department of Agriculture; S is the maximum retention of soil; CN is the curve number determined by land cover and soil type; CN_s is the modified curve number by slope; and $slope$ is the slope.

The data source applied for the modified SCS-CN model can be found in Supplementary Materials S1.

2.3.3. Habitat Quality

Green spaces purvey habitat services for organisms. However, urban expansion inevitably results in habitat loss and fragmentation, in turn leading to biodiversity loss. The HQ, quantified by the InVEST model, is frequently used in biodiversity assessment [58]. The InVEST model can output the HQ with better spatial visualization. This enables us to identify areas where the habitats are experiencing degradation due to built-up land encroachment and further evaluate the ToE between the degradation and the return of urbanization. The parameter settings of the InVEST model and the quantification of the HQ are detailed in Supplementary Materials S2.

2.3.4. Carbon Sequestration

Green spaces are important sites for CS and play a significant role in slowing down global warming and achieving carbon neutrality [59]. Built-up land expansion, however, may jeopardize terrestrial CS capacity [60]. Net primary productivity is the total amount of organic material produced by plants through photosynthesis minus the organic material consumed by the plants' respiration in an ecosystem, and the process essentially represents CS. We apply the NPP conversion method to quantify this ecological opportunity cost, as expressed by Equation (6).

$$CS = NPP \times \alpha \quad (6)$$

where CS is the amount of carbon sequestration; α is the conversion coefficient between net primary productivity and CO₂, equal to 1.63 based on the estimated carbon content in plant biomass [61]. The net primary productivity refers to GLASS Product suite [62], and its data source can be found in Supplementary Materials S1.

2.3.5. Data Normalization

From a return on investment perspective, UHI and FRS (runoff depth) serve as positive indicators, where higher values correspond to worse ecological conditions and greater ecological opportunity cost. In contrast, HQ and CS are negative indicators, with higher values suggesting better ecological conditions and lower opportunity cost. Therefore, these indicators with different directions need to be normalized to represent ecological degradation. It should be noted that in the SBM model, a non-parametric model used for measuring relative efficiency, linear transformation has no impact on the results. The former two positive indicators were normalized using Equation (7), while HQ and CS were normalized using Equation (8).

$$X_p = \frac{X_i - X_{\min}}{X_{\max} - X_{\min}} \quad (7)$$

$$X_n = \frac{X_{\max} - X_i}{X_{\max} - X_{\min}} \quad (8)$$

where X_p and X_n are the normalized values for positive and negative indicators, respectively; X_i is the value of the i th assessment unit; and X_{\max} and X_{\min} are the maximum and minimum value across the three periods.

2.4. Quantification of Urban Land Use Efficiency

ULUE can be spatially evaluated at a finer resolution by combining geospatial data, overcoming the limitations of traditional land use efficiency assessment methods that are conducted at the county level [63]. The carrying capacity of the population and the economic output are two crucial elements in the effectiveness of built-up land, and they are commonly used to quantify the ULUE [51]. Referring to Guo et al. [50] and Lu et al. [64], this study quantified ULUE using area-weighted nighttime light and population density

layers, shown in Equations (9)–(12). These two indices enabled us to assess the extent of artificial utilization of urbanized areas with visible human activities, which is a “white box” method. The ULUE is normalized with respect to the maximum value to facilitate direct comparison across three periods. ULUE is a positive variable and the higher ULUE corresponds to the greater effectiveness of the built-up land.

$$NTL_i = \sum_{m=1}^k NTL_m/k \quad (9)$$

$$Pop_i = \sum_{m=1}^k Pop_m/k \quad (10)$$

$$ULUE_i = NTL_i \times Pop_i \quad (11)$$

where NTL_i and Pop_i represent the nighttime light and population density of the i th assessment unit, respectively; NTL_m and Pop_m are the nighttime light and population density of the m th built-up land pixel; and k is the count of built-up land pixels within the i th assessment unit. $ULUE_i^n$ is the normalized urban land use efficiency of the i th assessment unit, while $ULUE_{max}$ is the maximum urban land use efficiency for the three periods. The nighttime light data refer to the harmonized global nighttime light dataset [65]; the population density is based on the WorldPop dataset. The data source can be found in Supplementary Materials S1.

2.5. Trade-Off Efficiency Evaluation: Slacks-Based Measure Model

The SBM model was first introduced by Tone, which is an improved form to the traditional Data Envelopment Analysis model [66]. The model directly introduces slack variables into the objective function in a non-radial manner, making it flexible and accurate in efficiency evaluation. Specifically, the model generates a production-possibility frontier based on input and output variables and calculates the distance that considers the slack improvement of each DMU to the frontier. The farther the distance, the lower the relative efficiency. In terms of proposed effectiveness trade-off between green spaces and built-up land, as well as the return on investment perspective, we set the ecological opportunity cost as input while the ULUE was the output. Additionally, 1 km² grids were set as the basic assessment units, which are the DMUs. A higher ToE indicates efficient urban–ecological linkage, with more socioeconomic output generated at lower ecological costs. The ToE quantified by the SBM model is shown below:

$$\rho = \min \frac{1 - \frac{1}{m} \sum_{i=1}^m s_i^- / x_{io}}{1 + \frac{1}{s} \sum_{r=1}^s s_r^+ / y_{ro}} \text{ s.t. } \begin{cases} x_0 = X\lambda + s^- \\ y_0 = Y\lambda - s^+ \\ s^- \geq 0 \\ s^+ \geq 0 \\ \lambda \geq 0 \\ \sum_{j=1, \neq 0}^n \lambda_j = 1 \end{cases} \quad (12)$$

where ρ is the ToE ranging from 0 to 1 and where 1 indicates full efficiency as well as desirable effectiveness trade-off between green spaces and built-up land; m , s and n are the number of inputs, output and DMUs, respectively; inputs and outputs are represented by two vectors: $x \in R^m$, $y \in R^s$; X is the input matrix, $X = [x_1, x_2 \cdots x_n] \in R^{n \times m}$, which contains the normalized ecological conditions for each assessment grid; Y is the output matrix, $Y = [y_1, y_2 \cdots y_n] \in R^{n \times s}$, which contains the normalized ULUE for each assessment grid; and s^- and s^+ are input and output slacks, respectively, and if the two variables

simultaneously equal 0, the DMUs are fully efficient. Otherwise, the DMUs are relatively inefficient, with a ToE value less than 1, demonstrating that these DMUs have room for improvement compared to the efficiency frontier in terms of input and output; that is, the assessment grids remain aspects to improve ULUE or ecological conditions.

2.6. Driver Detection for Trade-Off Efficiency

This study evaluates ToE on equal-area assessment units (1 km² grids). The equal-area-based evaluation neglects the quality factors, such as landscape pattern, NDVI (quality of green spaces), and building height (quality of built-up land), which could be drivers for the regional difference in ToE. Therefore, we used the geo-detector to explore the quality influencing factors to ToE in 2020. This is a spatial statistical model that detects the relative influence of driving factors on the target variable through the q -value (ranging from 0 to 1), where a larger q -value indicates stronger explanatory power. This tool also includes an interaction detector, which can identify whether the combined influence of two factors is enhanced or weakened compared to their individual effects [67].

The equation of the factor detector is as follows:

$$q = 1 - \frac{1}{N\sigma^2} \sum_{h=1}^L N_h \sigma_h^2 \quad (13)$$

where q is the explanatory ability of drivers; L is the number of categories; N_h and N are the number of units in layer h and the entire region, respectively; and σ^2 is the variance of the indicator. The q -values range from 0 to 1, and the higher the q -value, the stronger explanatory ability for spatial heterogeneity.

The interaction detector assesses how the interactive effect of a pair of drivers impacts the explanatory ability for the dependent variable, or whether these factors have independent impacts on the dependent variable [68]. This step is conducted by calculating the q -value for each individual indicator and the q -value for the interaction between the two indicators. Then, by comparing the individual indicator $q(X_1)$ and $q(X_2)$, and the interactive couple $q(X_1 \cap X_2)$, we can evaluate the level of their interactive effect.

Twelve landscape indices were initially selected based on the ecological significance in three aspects of fragmentation, shape, and aggregation of patches. We applied the moving window approach in Fragstats software (version 4.2) to spatially analyze these landscape indices. We tested window sizes of 60 m, 90 m, 120 m, 150 m, and 180 m. Among these, the 150 m window size provided a visually smooth representation, making it the preferred scale for subsequent analysis. Then, we conducted the multicollinearity test and finally retained number of patches (NPs), landscape shape index (LSI) and patch cohesion index (Cohesion) with variance inflation factor values < 7.5. Moreover, we selected the NDVI and mean building height as the quality indicators of green spaces and built-up land. The distance to water bodies was used to analyze the contribution of blue infrastructure to the ToE.

3. Results

3.1. Spatiotemporal Variations in Ecological Conditions

Figure 3a–l present the spatiotemporal variations in urban ecological conditions. We employed the Jenks natural break point method to categorize them into five degrees for uniform comparison across the three periods.

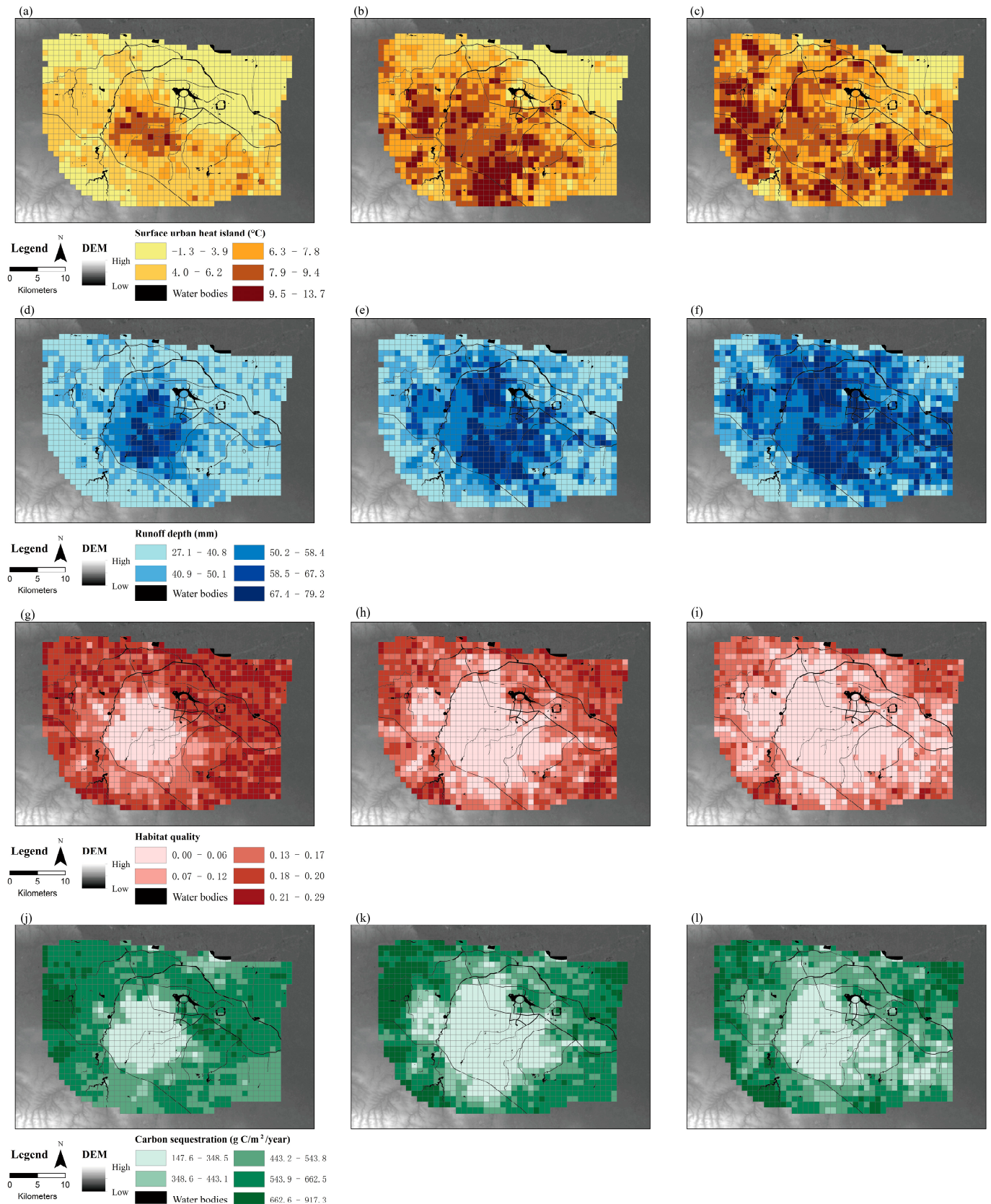


Figure 3. Urban–ecological conditions; (a–c) are urban heat islands in 2000, 2010, and 2020, respectively; (d–f) are flood regulating services (runoff depth) in 2000, 2010, and 2020, respectively; (g–i) are the habitat quality in 2000, 2010, and 2020, respectively; and (j–l) are the carbon sequestration in 2000, 2010, and 2020, respectively.

3.1.1. Spatiotemporal Pattern of Urban Heat Island

The analysis of UHI patterns for the three periods (Figure 3a–c) reveals pronounced temporal variations with significant spatial heterogeneity. In 2000, the highest UHI level (9.5–13.7) was primarily clustered within the urban core area, and the thermal environment was more desirable in the periphery. The higher UHI levels spread from the inner city to outside afterwards. In 2020, in particular, the UHI presented a polycentric trend, with the highest levels more dispersed around the outskirts, while the situation was slightly alleviated in the core area. In general, the UHI showed an upward trend, with the most severe thermal environment observed in 2020.

3.1.2. Spatiotemporal Pattern of Flood Regulating Service

Figure 3d–f reveal the spatiotemporal variations in FRS, where higher runoff depths indicate worse flood regulating conditions. The higher the runoff depth, the worse the flooding regulating service. There is a similar spatial pattern across the three periods. The better FRS was mainly aggregated around the surroundings, while the worse condition was mostly concentrated in the city center, where the runoff depth was above 58.5 mm for the 20-year rainfall return period. With urban sprawl, the peripheral FRS has aggravated. In 2000, the outlying areas generally provided optimal FRS with runoff depths of 26.8–40.8 mm, while only a few areas offered optimal flood control service in 2020 in the northeast and southwest ecological zones. Overall, the FRS has significantly deteriorated with urban expansion over the last two decades.

3.1.3. Spatiotemporal Pattern of Habitat Quality

HQ exhibited distinct spatial patterns across the study period (Figure 3g–i) and generally decreased from the inside to the outside, showing a similar spatial pattern across the three periods. The superior HQ level (0.21–0.29) was mostly scattered around the periphery in 2000 and 2010, while this level occupied a very small proportion in 2020, sporadically distributed around the ecological zone in the northeastern and southwestern edges. Overall, due to the rapid urban development, the general level of HQ has obviously declined since 2000, and most areas had the lowest HQ level of 0–0.06 in 2020.

3.1.4. Spatiotemporal Pattern of Carbon Sequestration

CS underwent notable changes (Figure 3j–l). The spatial pattern of CS was generally comparable across the three periods, increasing from the city heart to the periphery, and the five levels of CS generally had even proportions. The highest CS capacity of 662.6–917.3 was mostly concentrated in the western tip for the first two periods, while it was relatively interspersed around the fringe in 2020. Overall, the CS level was most desirable in 2000, reached its lowest level in 2010, and showed relative improvement in 2020, displaying a U-shaped trend.

3.2. Spatiotemporal Variations in Urban Land Use Efficiency

The spatiotemporal variations in ULUE are illustrated in Figure 4a–c. There is a comparable spatial pattern of ULUE across the three periods, generally decreasing from the inner city outwards. In 2000, the higher ULUE existed only in the inner city with a smaller area, while the ULUE in the outer city mostly showed the lowest level of 0.05–0.15. With the encroachment of built-up land on green spaces, the ULUE improved in 2010, although a few spots in the inner city showed a downward trend and there were still numerous areas with lower ULUE in the periphery. The overall ULUE was significantly enhanced in 2020, where quarters with higher were more scattered in the outskirts rather than concentrated within the inner city, demonstrating a polycentric development pattern. As a whole, ULUE

has increased significantly over the past two decades, and the improvement in the period of 2010–2020 is more pronounced than in the period of 2000–2010, suggesting that the growth speed of the city is accelerating.

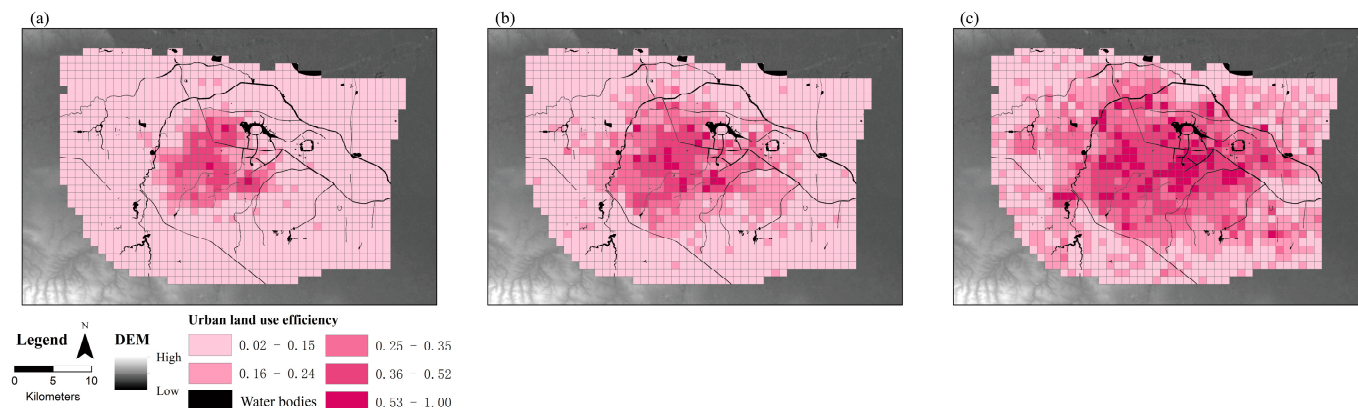


Figure 4. Urban land use efficiency: (a) 2000, (b) 2010, (c) 2020.

3.3. Spatiotemporal Variations in Trade-Off Efficiency and Descriptive Statistics

The spatiotemporal patterns of ToE are illustrated in Figure 5a–c, while their statistical distributions across the three periods are visualized through violin plots in Figure 6. The direction of ToE changes for each assessment unit during 2000–2010 and 2010–2020 is quantified in Figure 7a and 7b, respectively.

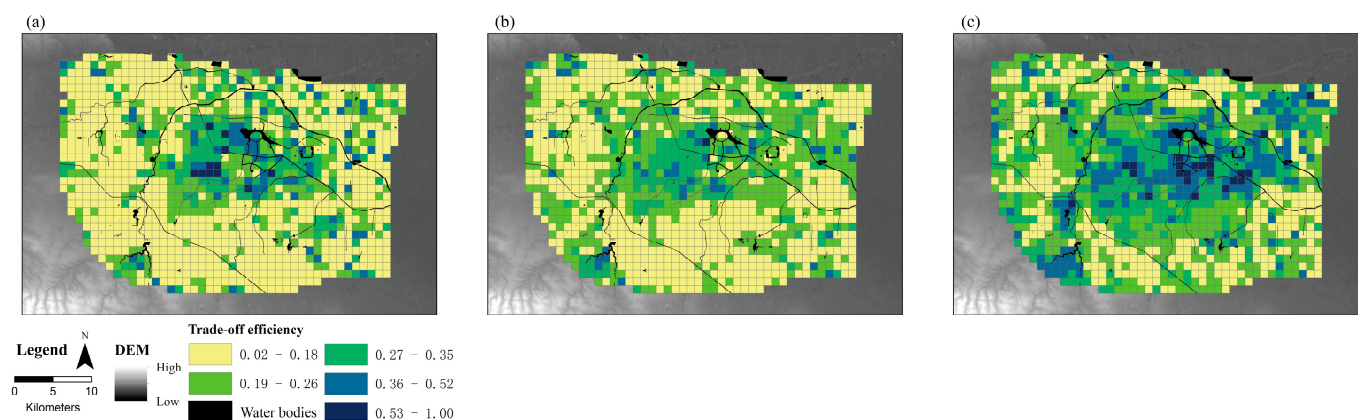


Figure 5. Spatial pattern of trade-off efficiency: (a) 2000, (b) 2010, (c) 2020.

The spatial pattern of ToE across the three periods is similar, with areas of higher ToE mainly aggregated within the inner city. Generally, ToE decreases from the inside to the outside. In 2000, ToE was the lowest among the three periods, with most spots showing the lowest levels of ToE outside the urban core area. By 2010, ToE had relatively improved, with the median and highest probability density of ToE increasing from 0.15 and 0.11 to 0.18 and 0.17, respectively. Despite the overall improvement, 37.1% of areas, primarily aggregated in the inner city and eastern tip, experienced a deterioration in ToE.

The improvement in ToE was more pronounced from 2010 to 2020 than from 2000 to 2010. The median and highest probability density of ToE increased to 0.24 and 0.22, respectively, compared to 2010. There are 78.8% of spots where ToE was improved, higher than the figure of 62.9% in the previous interval. In 2020, areas with lower ToE were mostly dispersed in the periphery. In contrast, spots within the inner city, sub-centers in the north, and adjacent to ecological zones such as water bodies, wetlands, and forests demonstrated desirable ToE. Notably, the highest ToE of 1 was observed in 2020 within the city center near Longhu Park, whereas the highest ToE was 0.63 in 2000 and 0.58 in 2010.

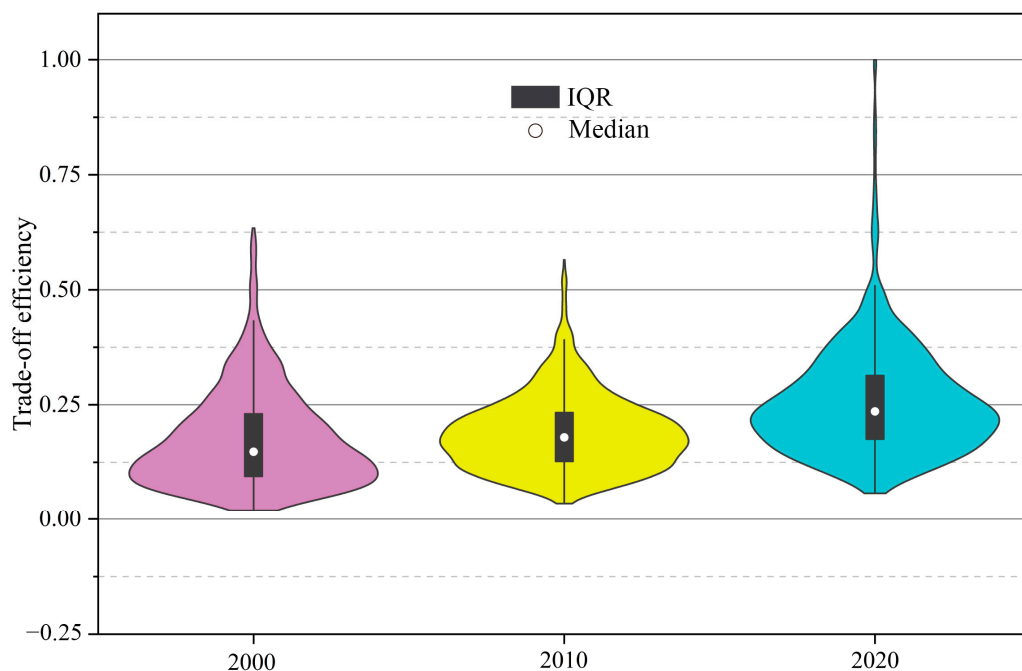


Figure 6. Distribution of trade-off efficiency.

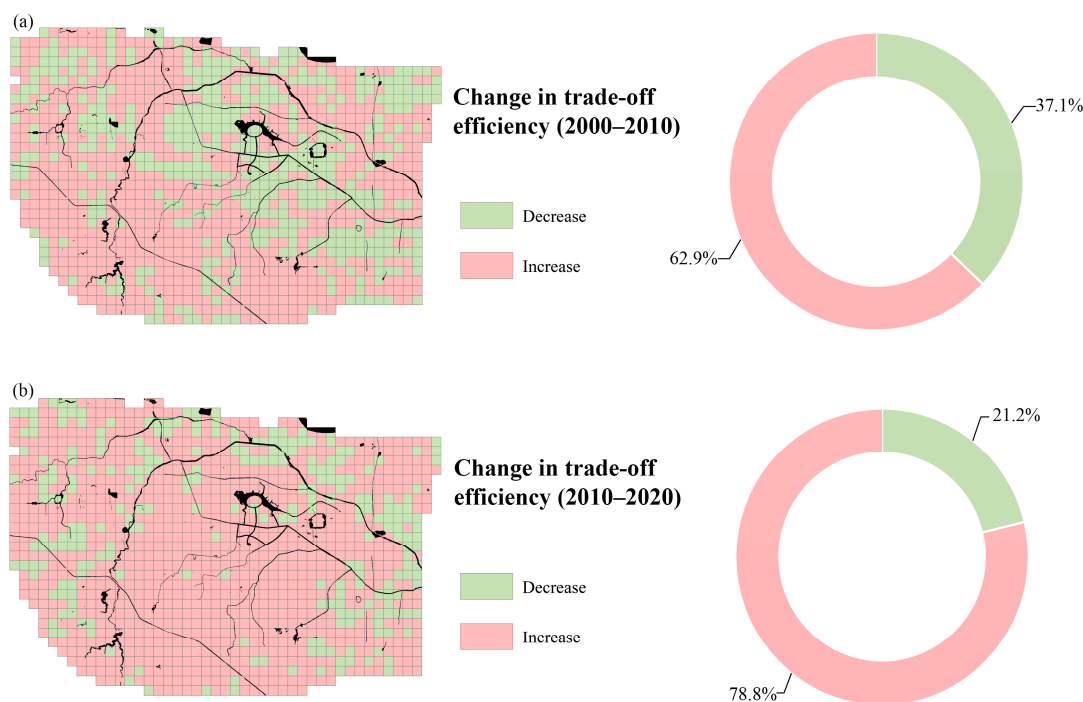


Figure 7. Spatiotemporal change in trade-off efficiency: (a) 2000–2010, (b) 2010–2020.

In short, ToE has significantly improved over the last two decades. However, in some areas, especially within the inner city, ToE initially decreased in 2010 and then increased in 2020, exhibiting a U-shaped trend, suggesting that the improvement is uneven, and spatial disparity remains prominent from a local perspective.

3.4. Driving Mechanism of Trade-Off Efficiency

The results of single-factor detection are shown in Table 1. Among the landscape indices, NP_gs, LSI_gs, NP_bl, and LSI_bl are not statistically significant, with p -values > 0.05 . Although the other two landscape indices, Cohesion_gs and Cohesion_bl, are significant,

their q -value is only 0.083 and 0.098, respectively. This suggests that, irrespective of green spaces or built-up land, their landscape patterns as single drivers have a slight impact on ToE.

Table 1. Result of single factor detector. Abbreviation: green spaces (gs); built-up land (bl).

	NP_gs (X1)	LSI_gs (X2)	Cohesion_gs (X3)	NP_bl (X4)	LSI_bl (X5)	Cohesion_bl (X6)	NDVI (X7)	Building Height (X8)	Distance to Water Bodies (X9)
q statistic	0.009	0.014	0.083	0.009	0.025	0.098	0.105	0.178	0.047
p value	0.332	0.121	0	0.28	0.126	0	0	0	0.007

Building height has a q -value of 0.178, indicating the highest explanatory power among the factors, followed by NDVI with an explanatory power of 0.105. The distance to water bodies also has less impact on ToE. In terms of single-factor detection, ToE is mostly impacted by the quality of green spaces and built-up land, that is, building height and NDVI, rather than landscape patterns and surrounding water bodies.

The interaction detection results are shown in Figure 8. The interaction detection reveals three different types of interaction effects: single-variable attenuation, dual-variable enhancement, and non-linear enhancement, with 4, 10, and 31 pairs, respectively. The most common interaction effect is non-linear enhancement, which demonstrates a significant synergistic effect between drivers on ToE, exemplifying the effect of $1 + 1 > 2$. For example, among the landscape indices, NP_gs, despite not having a significant effect as a single driver, shows the most significant synergistic effect with Cohesion_bl, with a q -value of 0.137 (X6∩X1). This synergistic effect suggests that simultaneously optimizing the landscape patterns of green spaces and built-up land could significantly improve ToE, compared to considering a single landscape class alone.

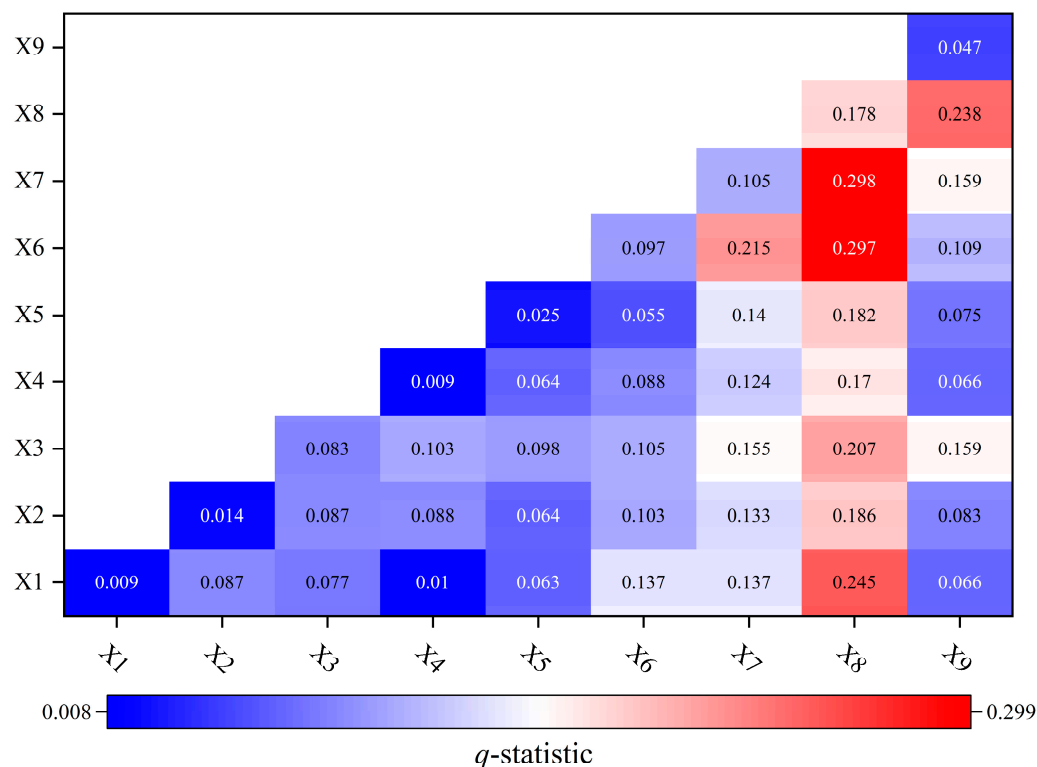


Figure 8. Result of interaction detection. Note: single-variable attenuation is $\text{Min}(q(X1), q(X2)) < q(X1 \cap X2) < \text{Max}(q(X1), q(X2))$; dual-variable enhancement is $q(X1 \cap X2) > \text{Max}(q(X1), q(X2))$; and non-linear enhancement is $q(X1 \cap X2) > q(X1) + q(X2)$.

Among all interaction effects, the highest explanatory power is found in the pair of NDVI and building height ($X8 \cap X7$) with a q -value of 0.298, followed by the combination of building height and Cohesion_bl ($X8 \cap X6$), and NP_gs ($X8 \cap X1$) with a q -value of 0.297 and 0.245, respectively. Notably, there is a weaker interaction between NP_bl and building height, suggesting that the fragmentation of built-up land undermines the impact of building height on ToE. Furthermore, distance to water bodies, despite having minor explanatory power as a single driver, shows a significant synergistic effect with NDVI ($X9 \cap X7$) and building height ($X9 \cap X8$). In general, the results of interaction detection imply that the green, gray and blue components are mutually reinforcing. Therefore, compared to isolating these components, most effective synergistic impacts on ToE might be achieved by optimizing them simultaneously.

4. Discussion

4.1. Reliability Test

As a rapidly expanding city and one of the major cities situated in the middle of the Yellow River basin, Zhengzhou's urban area has undergone rapid expansion, accompanied by various ecological issues, such as UHI, flooding risk and biodiversity loss, etc. [69–71]. Given its representative characteristics and ecological challenges, the city's spatiotemporal trends of urban expansion and urban–ecological conditions have been monitored by many scholars. In this section, the identified ULUE and urban–ecological conditions are compared with the existing literature.

Several city-level land use efficiency studies using official statistical data have shown that Zhengzhou's ULUE has experienced a pronounced improvement over the past two decades [72–74]. Although these studies used different methods, they reported trends that were consistent with our findings.

Zhou et al. [75] demonstrated that although the mean land surface temperature increased by 0.92 °C from 2005 to 2020, the spatial pattern of the UHI changed significantly and became irregularly distributed. Similarly, Yang et al. [76] indicated that the UHI pattern in Zhengzhou experienced overall exacerbation and spatial variations from 2000 to 2020. These two features of the UHI highlighted in previous studies are in line with our results. Guoyi et al. [77] employed GIS and Analytic Hierarchy Process methods and substantiated that urban flood risk in Zhengzhou expanded from 2000 to 2020 with urbanization. This finding was corroborated by Dai et al. [69], who showed an increased flood risk and deteriorated flood regulating capacity due to impervious land expansion, consistent with our study. The HQ in Zhengzhou has also experienced overall degradation due to urban expansion over the past two decades, as reported by Zhao et al. [71] and Zheng et al. [78]. These findings are similar to ours.

Since 2013, the Zhengzhou government has initiated the forest city program to restore ecological degradation. These projects have yielded positive outcomes, as many studies indicated improvements in both vegetation cover and NDVI values within the inner city [76,79,80], suggesting a spatiotemporal trend of enhanced CS. Furthermore, the ToE within the inner city first decreased and then increased by 2020, which could also be ascribed to the restoration measure. In summary, the identified ecological conditions and ULUE in this study are credible and in accordance with previous studies and the city's greening project.

4.2. Advancements Beyond Traditional Methods

The evaluation of the urban–ecological linkage has attracted growing attention from urban planners, policymakers, and scholars. This study presents a return on investment-based perspective on the urban–ecological relationship by linking the effectiveness trade-off

between green spaces and built-up land. This framework provides theoretical support for evaluating the urban–ecological linkage and offers justification for the selection of associated indicators. This justification distinguishes it from traditional studies that subjectively choose evaluation metrics and assign their weights without theoretical basis [81]. ToE varies depending on the effectiveness of the replaced green spaces and the newly developed built-up land. This linkage helps determine whether urban expansion encroaches on highly valuable green spaces or whether the development is inefficient and results in wasted land resources. Specifically, if urban expansion encroaches green spaces providing substantial ecological effectiveness, the ToE would be undermined compared to encroachment on bare and unused land, which usually has less ecological effectiveness. On the other hand, if urban land use is extensive, it would contribute less socio-economic output at given areas. This cause of lower ToE is evident in the first period of 2000 in the outskirts, where a large number of villages with extensive land use clustered beyond the inner city.

Furthermore, this study can be conducted at a resolution of 1 km², which is much finer than previous studies conducted at the county level or larger scales [35]. According to the fundamental principles of spatial analysis, research conducted at a finer resolution can be replicated at a coarser scale, whereas the reverse is not feasible. Moreover, the comprehensive urban–ecological quality and ULUE are quantified primarily using open-source data rather than locally specific statistical data as applied in previous approaches. This allows for easy replication of the evaluation model in other cities worldwide and facilitates uniform comparisons between cities in different countries.

4.3. Planning and Policy Implications

Although ToE has improved over the last two decades, the difference along the urban–rural gradient remains pronounced. The lower ToE in the periphery is primarily due to extensive land use, while the inner city is hampered by inferior ecological quality. Therefore, strategies to enhance ToE should be tailored accordingly.

In the urban periphery, the primary goal should be improving ULUE and curbing irrational urban sprawl. Many areas with higher ToE are adjacent to water bodies, wetlands, and forest parks, highlighting the critical role of these ecological areas in providing additional ecosystem services to their surroundings. Hence, it is imperative to avoid encroaching on highly efficient ecological land and to eschew a development pathway of first destruction and then restoration. Instead, urban development should be coordinated with these ecologically conducive factors to facilitate better access to ecosystem services so as to improve surrounding residents' health and well-being [82,83].

In the inner city, ecological restoration should be prioritized. Interaction detection, such as pairs of height and NDVI, and NP_gs and Cohesion_bl, highlights the necessity of targeted high-quality green infrastructure interventions (e.g., NDVI) in highly urbanized areas to synergistically improve ToE. Given the higher development density and fewer open spaces, small and centralized green infrastructure can be implemented in areas suffering from specific ecological issues. For example, trees with a lower crown temperature are effective in microclimate regulation and can be planted as urban tree canopies as a targeted response to the UHI [84]. Similarly, small stormwater ponds with high runoff retention and infiltration effectiveness can be targeted in areas with poor hydrological performance to alleviate flood pressure [85].

4.4. Limitations and Future Directions

Although this study quantifies urban–ecological conditions through four aspects—UHI, FRS, HQ, and CS—it remains insufficient compared to the full range of benefits that green spaces can provide. Future research should incorporate additional ecological elements such

as soil retention, insect diversity, and pollination to present a more comprehensive view of the urban–ecological condition. Additionally, despite their lower impact on urban–ecological conditions, provisioning and cultural services are also crucial for human survival and well-being. Therefore, future studies could broaden the dimension of the framework to provide a more holistic assessment by integrating the other culturally effective aspects of green spaces, such as esthetic value and recreation.

The application of the SBM model and geo-detector also has a few limitations. The SBM model assumes linear relationships between inputs and outputs, which may not fully reflect the complex, non-linear nature of urban–ecological interactions. Meanwhile, the geo-detector results are sensitive to the classification of numerical variables and the spatial scale of analysis units. Future research could explore more sophisticated methods to address these limitations.

The proposed framework could also be extended to cities with diverse attributes, including cities in different countries, cities in developing states, and cities of various scales and geographical locations. This would enhance understanding of the drivers and optimization pathways for ToE.

5. Conclusions

In this study, we introduce a distinct perspective on evaluating the urban–ecological relationship by linking the effectiveness between green spaces and built-up land from a return on investment perspective. Our findings reveal that the urban–ecological conditions in Zhengzhou’s periphery significantly degraded over the past two decades, while an improvement trend in UHI and CS was observed within the inner city. ULUE experienced a pronounced improvement, particularly in the second phase (2010–2020). ToE generally showed an upward trend, while certain areas within the inner city experienced an initial decline followed by an increase. Factor detection indicates that building height and NDVI have the highest explanatory power, with q -values of 0.178 and 0.105, respectively. Interaction detection reveals significant synergistic effects between pairs of drivers, such as NDVI and building height, and NP_gs and Cohesion_bl, with q -values of 0.298 and 0.137, respectively.

Based on the findings, we propose planning and policy suggestions. In the outskirts, the primary tasks should focus on optimizing urban form to strengthen intensive land use and coordinate with ecologically conducive factors to facilitate better access to ecosystem services. The pathway of first destruction and then restoration should be eschewed, whereas in urban core areas, small and centralized green infrastructure with higher quality (NDVI) should be targeted in areas suffering from specific ecological issues given the synergistic effect between gray and green factors. The developed framework could serve as a guide to assist decision-makers and urban planners in monitoring urban–ecological conditions and developing adaptive planning strategies to enhance urban sustainability in the context of urban expansion.

Supplementary Materials: The following supporting information can be downloaded at: <https://www.mdpi.com/article/10.3390/rs17020212/s1>, Supplementary Materials S1: Data acquisition; Table S1: Data acquisition list; Supplementary Materials S2: Quantification of habitat quality; Table S2: Threat sources for quantification of habitat quality; Table S3: Sensitivity of land use to threat sources.

Author Contributions: Conceptualization, X.D.; methodology, X.D.; software, X.D. and T.Z.; validation, X.D. and T.Z.; formal analysis, X.D.; investigation, X.D.; resources, T.Z.; data curation, X.D.; writing—original draft preparation, X.D.; writing—review and editing, Y.Y., D.H. and A.L.; visualization, X.D.; supervision, Y.Y., D.H. and A.L.; project administration, Y.Y.; funding acquisition, Y.Y. All authors have read and agreed to the published version of the manuscript.

Funding: Major Projects of the National Social Science Foundation of China (19ZDA088) and National Natural Science Foundation of China Projects (42071250).

Data Availability Statement: Dataset available on request from the authors.

Conflicts of Interest: The authors declare no conflict of interest.

References

- World Population Review. Most Urbanized Countries 2023. Available online: <https://worldpopulationreview.com/country-rankings/most-urbanized-countries> (accessed on 30 November 2023).
- NBSC. 7th National Population Census. National Bureau of Statistics of China. 2021. Available online: https://www.gov.cn/guoqing/2021-05/13/content_5606149.htm (accessed on 30 December 2021).
- Knight, S.J.; McClean, C.J.; White, P.C.L. The importance of ecological quality of public green and blue spaces for subjective well-being. *Landsc. Urban Plan.* **2022**, *226*, 104510. [[CrossRef](#)]
- Peng, J.; Qiao, R.; Wang, Q.; Yu, S.; Dong, J.; Yang, Z. Diversified evolutionary patterns of surface urban heat island in new expansion areas of 31 Chinese cities. *npj Urban Sustain.* **2024**, *4*, 14. [[CrossRef](#)]
- Yue, Z.; Xiao, C.; Feng, Z.; Wang, Y.; Yan, H. Accelerating decline of habitat quality in Chinese border areas. *Resour. Conserv. Recycl.* **2024**, *206*, 107665. [[CrossRef](#)]
- Kabisch, N.; Haase, D. Green spaces of European cities revisited for 1990–2006. *Landsc. Urban Plan.* **2013**, *110*, 113–122. [[CrossRef](#)]
- Pauleit, S.; Lindley, S.; Cilliers, S.; Shackleton, C. Urbanisation and ecosystem services in sub-Saharan Africa: Current status and scenarios. *Landsc. Urban Plan.* **2018**, *180*, 247–248. [[CrossRef](#)]
- Raymond, C.M.; Frantzeskaki, N.; Kabisch, N.; Berry, P.; Breil, M.; Nita, M.R.; Geneletti, D.; Calfapietra, C. A framework for assessing and implementing the co-benefits of nature-based solutions in urban areas. *Environ. Sci. Policy* **2017**, *77*, 15–24. [[CrossRef](#)]
- Frantzeskaki, N.; McPhearson, T.; Collier, M.J.; Kendal, D.; Bulkeley, H.; Dumitru, A.; Walsh, C.; Noble, K.; van Wyk, E.; Ordóñez, C.; et al. Nature-Based Solutions for Urban Climate Change Adaptation: Linking Science, Policy, and Practice Communities for Evidence-Based Decision-Making. *BioScience* **2019**, *69*, 455–466. [[CrossRef](#)]
- Xue, B.; Han, B.; Li, H.; Gou, X.; Yang, H.; Thomas, H.; Stückrad, S. Understanding ecological civilization in China: From political context to science. *Ambio* **2023**, *52*, 1895–1909. [[CrossRef](#)] [[PubMed](#)]
- Nguyen, T.T.; Ngo, H.H.; Guo, W.; Wang, X.C. A new model framework for sponge city implementation: Emerging challenges and future developments. *J. Environ. Manag.* **2020**, *253*, 109689. [[CrossRef](#)] [[PubMed](#)]
- Shao, J.; Ge, J. Investigation into Relationship between Intensive Land Use and Urban Heat Island Effect in Shijiazhuang City Based on the Tapio Decoupling Theory. *J. Urban Plan. Dev.* **2020**, *146*, 04020043. [[CrossRef](#)]
- Wu, T.; Liu, Y.; Qi, X.; Zhang, Q.; Yao, Y.; Wu, J. The environmental impact assessment of China’s ecological migration from a social–ecological perspective. *Ambio* **2024**, *53*, 1355–1366. [[CrossRef](#)]
- Zhang, Z.; Zhao, W.; Liu, Y.; Pereira, P. Impacts of urbanisation on vegetation dynamics in Chinese cities. *Environ. Impact Assess. Rev.* **2023**, *103*, 107227. [[CrossRef](#)]
- Wang, Y.; van Vliet, J.; Debonne, N.; Pu, L.; Verburg, P.H. Settlement changes after peak population: Land system projections for China until 2050. *Landsc. Urban Plan.* **2021**, *209*, 104045. [[CrossRef](#)]
- Standish, R.J.; Hobbs, R.J.; Miller, J.R. Improving city life: Options for ecological restoration in urban landscapes and how these might influence interactions between people and nature. *Landsc. Ecol.* **2013**, *28*, 1213–1221. [[CrossRef](#)]
- Ran, P.; Frazier, A.E.; Xia, C.; Tiando, D.S.; Feng, Y. How does urban landscape pattern affect ecosystem health? Insights from a spatiotemporal analysis of 212 major cities in China. *Sustain. Cities Soc.* **2023**, *99*, 104963. [[CrossRef](#)]
- Sarker, T.; Fan, P.; Messina, J.P.; Mujahid, N.; Aldrian, E.; Chen, J. Impact of Urban built-up volume on Urban environment: A Case of Jakarta. *Sustain. Cities Soc.* **2024**, *105*, 105346. [[CrossRef](#)]
- Tratalos, J.; Fuller, R.A.; Warren, P.H.; Davies, R.G.; Gaston, K.J. Urban form, biodiversity potential and ecosystem services. *Landsc. Urban Plan.* **2007**, *83*, 308–317. [[CrossRef](#)]
- Zhang, D.; Huang, Q.; He, C.; Wu, J. Impacts of urban expansion on ecosystem services in the Beijing–Tianjin–Hebei urban agglomeration, China: A scenario analysis based on the Shared Socioeconomic Pathways. *Resour. Conserv. Recycl.* **2017**, *125*, 115–130. [[CrossRef](#)]
- Qu, H.; You, C.; Wang, W.; Guo, L. Spatio-temporal interplay between ecosystem services and urbanization in the Yangtze River Economic Belt: A new perspective for considering the scarcity effect. *Land Use Policy* **2024**, *147*, 107358. [[CrossRef](#)]
- Guo, X.; Shahbaz, M. The existence of environmental Kuznets curve: Critical look and future implications for environmental management. *J. Environ. Manag.* **2024**, *351*, 119648. [[CrossRef](#)]
- Li, K.; Hou, Y.; Randall, M.T.; Skov-Petersen, H.; Li, X. The spatio-temporal trade-off between ecosystem and basic public services and the urbanization driving force in the rapidly urbanizing region. *Sustain. Cities Soc.* **2024**, *111*, 105554. [[CrossRef](#)]

24. Liao, Q.; Li, T.; Wang, Q.; Liu, D. Exploring the ecosystem services bundles and influencing drivers at different scales in southern Jiangxi, China. *Ecol. Indic.* **2023**, *148*, 110089. [[CrossRef](#)]
25. Robaina, M.; Rodrigues, S.; Madaleno, M. Is there a trade-off between human well-being and ecological footprint in European countries? *Ecol. Econ.* **2024**, *224*, 108296. [[CrossRef](#)]
26. Briones-Hidrovo, A.; Uche, J.; Martínez-Gracia, A. Estimating the hidden ecological costs of hydropower through an ecosystem services balance: A case study from Ecuador. *J. Clean. Prod.* **2019**, *233*, 33–42. [[CrossRef](#)]
27. Pirmana, V.; Alisjahbana, A.S.; Yusuf, A.A.; Hoekstra, R.; Tukker, A. Environmental costs assessment for improved environmental-economic account for Indonesia. *J. Clean. Prod.* **2021**, *280*, 124521. [[CrossRef](#)]
28. Halder, B.; Bandyopadhyay, J.; Banik, P. Monitoring the effect of urban development on urban heat island based on remote sensing and geo-spatial approach in Kolkata and adjacent areas, India. *Sustain. Cities Soc.* **2021**, *74*, 103186. [[CrossRef](#)]
29. Kasim, O.F.; Wahab, B.; Oweniwe, M.F. Urban expansion and enhanced flood risk in Africa: The example of Lagos. *Environ. Hazards* **2022**, *21*, 137–158. [[CrossRef](#)]
30. Sun, B.; Fang, C.; Liao, X.; Guo, X.; Liu, Z. The relationship between urbanization and air pollution affected by intercity factor mobility: A case of the Yangtze River Delta region. *Environ. Impact Assess. Rev.* **2023**, *100*, 107092. [[CrossRef](#)]
31. Boori, M.S.; Choudhary, K.; Paringer, R.; Kupriyanov, A. Eco-environmental quality assessment based on pressure-state-response framework by remote sensing and GIS. *Remote Sens. Appl. Soc. Environ.* **2021**, *23*, 100530. [[CrossRef](#)]
32. Leka, A.; Lagarias, A.; Panagiotopoulou, M.; Stratigea, A. Development of a Tourism Carrying Capacity Index (TCCI) for sustainable management of coastal areas in Mediterranean islands—Case study Naxos, Greece. *Ocean Coast. Manag.* **2022**, *216*, 105978. [[CrossRef](#)]
33. Zhang, D.; Chen, Y. Evaluation on urban environmental sustainability and coupling coordination among its dimensions: A case study of Shandong Province, China. *Sustain. Cities Soc.* **2021**, *75*, 103351. [[CrossRef](#)]
34. Liu, J.; Jin, X.; Li, H.; Zhang, X.; Xu, W.; Fan, Y.; Zhou, Y. Spatial-temporal changes and driving factors of the coordinated relationship among multiple land use efficiencies integrating stakeholders' vision in eastern China. *J. Clean. Prod.* **2022**, *336*, 130406. [[CrossRef](#)]
35. Luo, W.; Bai, H.; Jing, Q.; Liu, T.; Xu, H. Urbanization-induced ecological degradation in Midwestern China: An analysis based on an improved ecological footprint model. *Resour. Conserv. Recycl.* **2018**, *137*, 113–125. [[CrossRef](#)]
36. Awotwi, A.; Anornu, G.K.; Quaye-Ballard, J.A.; Annor, T. Monitoring land use and land cover changes due to extensive gold mining, urban expansion, and agriculture in the Pra River Basin of Ghana, 1986–2025. *Land Degrad. Dev.* **2018**, *29*, 3331–3343. [[CrossRef](#)]
37. Leng, A.; Wang, K.; Bai, J.; Gu, N.; Feng, R. Analyzing sustainable development in Chinese cities: A focus on land use efficiency in production-living-ecological aspects. *J. Clean. Prod.* **2024**, *448*, 141461. [[CrossRef](#)]
38. Grafius, D.R.; Corstanje, R.; Harris, J.A. Linking ecosystem services, urban form and green space configuration using multivariate landscape metric analysis. *Landsc. Ecol.* **2018**, *33*, 557–573. [[CrossRef](#)]
39. Hami, A.; Abdi, B.; Zarehaghi, D.; Maulan, S.B. Assessing the thermal comfort effects of green spaces: A systematic review of methods, parameters, and plants' attributes. *Sustain. Cities Soc.* **2019**, *49*, 101634. [[CrossRef](#)]
40. Trabucchi, M.; O'Farrell, P.J.; Notivol, E.; Comín, F.A. Mapping Ecological Processes and Ecosystem Services for Prioritizing Restoration Efforts in a Semi-arid Mediterranean River Basin. *Environ. Manag.* **2014**, *53*, 1132–1145. [[CrossRef](#)] [[PubMed](#)]
41. Vrebos, D.; Staes, J.; Vandenbroucke, T.; D'Haeyer, T.; Johnston, R.; Muhumuza, M.; Kasabeke, C.; Meire, P. Mapping ecosystem service flows with land cover scoring maps for data-scarce regions. *Ecosyst. Serv.* **2015**, *13*, 28–40. [[CrossRef](#)]
42. Basu, T.; Das, A.; Das, K.; Pereira, P. Urban expansion induced loss of natural vegetation cover and ecosystem service values: A scenario-based study in the siliguri municipal corporation (Gateway of North-East India). *Land Use Policy* **2023**, *132*, 106838. [[CrossRef](#)]
43. Mahtta, R.; Fragkias, M.; Güneralp, B.; Mahendra, A.; Reba, M.; Wentz, E.A.; Seto, K.C. Urban land expansion: The role of population and economic growth for 300+ cities. *npj Urban Sustain.* **2022**, *2*, 5. [[CrossRef](#)]
44. Yoo, C.; Xiao, H.; Zhong, Q.-w.; Weng, Q. Unequal impacts of urban industrial land expansion on economic growth and carbon dioxide emissions. *Commun. Earth Environ.* **2024**, *5*, 203. [[CrossRef](#)]
45. Xia, Z.; Huang, J.; Huang, Y.; Liu, K.; Zhu, R.; Shen, Z.; Yuan, C.; Liu, L. A social-ecological approach for identifying and mapping ecosystem service trade-offs and conservation priorities in peri-urban areas. *Ambio* **2024**, *53*, 1522–1540. [[CrossRef](#)] [[PubMed](#)]
46. Wang, S.; Hu, M.; Wang, Y.; Xia, B. Dynamics of ecosystem services in response to urbanization across temporal and spatial scales in a mega metropolitan area. *Sustain. Cities Soc.* **2022**, *77*, 103561. [[CrossRef](#)]
47. Zhang, Q.; Yang, L.; Xu, S. The Relationships of Supporting Services and Regulating Services in National Forest City. *Forests* **2022**, *13*, 1368. [[CrossRef](#)]
48. Cortinovis, C.; Geneletti, D. A framework to explore the effects of urban planning decisions on regulating ecosystem services in cities. *Ecosyst. Serv.* **2019**, *38*, 100946. [[CrossRef](#)]

49. Hack, J.; Molewijk, D.; Beißler, M.R. A Conceptual Approach to Modeling the Geospatial Impact of Typical Urban Threats on the Habitat Quality of River Corridors. *Remote Sens.* **2020**, *12*, 1345. [CrossRef]
50. Guo, X.; Chen, Y.; Jia, Z.; Li, Y.; Zhang, L.; Qiao, Z.; Hao, Y. Spatial and temporal inequity of urban land use efficiency in China: A perspective of dynamic expansion. *Environ. Impact Assess. Rev.* **2024**, *104*, 107357. [CrossRef]
51. Schiavina, M.; Melchiorri, M.; Freire, S.; Florio, P.; Ehrlich, D.; Tommasi, P.; Pesaresi, M.; Kemper, T. Land use efficiency of functional urban areas: Global pattern and evolution of development trajectories. *Habitat Int.* **2022**, *123*, 102543. [CrossRef] [PubMed]
52. Rajagopal, P.; Priya, R.S.; Senthil, R. A review of recent developments in the impact of environmental measures on urban heat island. *Sustain. Cities Soc.* **2023**, *88*, 104279. [CrossRef]
53. Schwarz, N.; Lautenbach, S.; Seppelt, R. Exploring indicators for quantifying surface urban heat islands of European cities with MODIS land surface temperatures. *Remote Sens. Environ.* **2011**, *115*, 3175–3186. [CrossRef]
54. USGS. Landsat 8-9 Collection 2 Level 2 Science Product Guide. 2024. Available online: <https://www.usgs.gov/media/files/landsat-8-9-collection-2-level-2-science-product-guide> (accessed on 30 November 2023).
55. Ren, T.; Zhou, W.; Wang, J. Beyond intensity of urban heat island effect: A continental scale analysis on land surface temperature in major Chinese cities. *Sci. Total Environ.* **2021**, *791*, 148334. [CrossRef] [PubMed]
56. Konduru, R.T.; Mrudula, G.; Singh, V.; Srivastava, A.K.; Singh, A.K. Unravelling the causes of 2015 winter monsoon extreme rainfall and floods over Chennai: Influence of atmospheric variability and urbanization on the hydrological cycle. *Urban Clim.* **2023**, *47*, 101395. [CrossRef]
57. Huang, M.; Gallichand, J.; Wang, Z.; Goulet, M. A modification to the Soil Conservation Service curve number method for steep slopes in the Loess Plateau of China. *Hydrol. Process.* **2006**, *20*, 579–589. [CrossRef]
58. Abolmaali, S.M.-r.; Tarkesh, M.; Mousavi, S.A.; Karimzadeh, H.; Pourmanafi, S.; Fakheran, S. Impacts of spatio-temporal change of landscape patterns on habitat quality across Zayanderud Dam watershed in central Iran. *Sci. Rep.* **2024**, *14*, 8780. [CrossRef] [PubMed]
59. Pereira, P.; Wang, F.; Inacio, M.; Kalinauskas, M.; Bogdzevič, K.; Bogunovic, I.; Zhao, W.; Barcelo, D. Nature-based solutions for carbon sequestration in urban environments. *Curr. Opin. Environ. Sci. Health* **2024**, *37*, 100536. [CrossRef]
60. Rani, V.; Schwing, P.T.; Jayachandran, P.R.; Preethy, C.M.; Sreelekshmi, S.; Joseph, P.; Bijoy Nandan, S. Carbon stocks and sequestration rate in mangroves and its major influencing factors from highly urbanised port city, southern India. *J. Environ. Manag.* **2023**, *335*, 117542. [CrossRef]
61. Jiang, H.; Peng, J.; Dong, J.; Zhang, Z.; Xu, Z.; Meersmans, J. Linking ecological background and demand to identify ecological security patterns across the Guangdong-Hong Kong-Macao Greater Bay Area in China. *Landsc. Ecol.* **2021**, *36*, 2135–2150. [CrossRef]
62. Yuan, W.; Zheng, Y.; Piao, S.; Ciais, P.; Lombardozzi, D.; Wang, Y.; Ryu, Y.; Chen, G.; Dong, W.; Hu, Z.; et al. Increased atmospheric vapor pressure deficit reduces global vegetation growth. *Sci. Adv.* **2019**, *5*, eaax1396. [CrossRef]
63. Ruan, L.; He, T.; Xiao, W.; Chen, W.; Lu, D.; Liu, S. Measuring the coupling of built-up land intensity and use efficiency: An example of the Yangtze River Delta urban agglomeration. *Sustain. Cities Soc.* **2022**, *87*, 104224. [CrossRef]
64. Lu, Y.; He, T.; Yue, W.; Li, M.; Shan, Z.; Zhang, M. Does cropland threaten urban land use efficiency in the peri-urban area? Evidence from metropolitan areas in China. *Appl. Geogr.* **2023**, *161*, 103124. [CrossRef]
65. Li, X.; Zhou, Y.; Zhao, M.; Zhao, X. A harmonized global nighttime light dataset 1992–2018. *Sci. Data* **2020**, *7*, 168. [CrossRef]
66. Tone, K. A slacks-based measure of super-efficiency in data envelopment analysis. *Eur. J. Oper. Res.* **2002**, *143*, 32–41. [CrossRef]
67. Zhai, Y.; Zhai, G.; Chen, Y.; Liu, J. Research on regional terrestrial carbon storage based on the pattern-process-function. *Ecol. Inform.* **2024**, *80*, 102523. [CrossRef]
68. He, X.; Zhou, Y. Urban spatial growth and driving mechanisms under different urban morphologies: An empirical analysis of 287 Chinese cities. *Landsc. Urban Plan.* **2024**, *248*, 105096. [CrossRef]
69. Dai, K.; Shen, S.; Cheng, C.; Song, Y. Integrated evaluation and attribution of urban flood risk mitigation capacity: A case of Zhengzhou, China. *J. Hydrol. Reg. Stud.* **2023**, *50*, 101567. [CrossRef]
70. Yang, H.; Wu, Z.; Dawson, R.J.; Barr, S.; Ford, A.; Li, Y. Quantifying surface urban heat island variations and patterns: Comparison of two cities in three-stage dynamic rural–urban transition. *Sustain. Cities Soc.* **2024**, *109*, 105538. [CrossRef]
71. Zhao, M.; Tian, Y.; Dong, N.; Hu, Y.; Tian, G.; Lei, Y. Spatial and temporal dynamics of habitat quality in response to socioeconomic and landscape patterns in the context of urbanization: A case in Zhengzhou City, China. *J. Nat. Conserv.* **2022**, *48*, 185–212. [CrossRef]
72. He, S.; Yu, S.; Li, G.; Zhang, J. Exploring the influence of urban form on land-use efficiency from a spatiotemporal heterogeneity perspective: Evidence from 336 Chinese cities. *Land Use Policy* **2020**, *95*, 104576. [CrossRef]
73. Li, H.; Wang, Z.; Zhu, M.; Hu, C.; Liu, C. Study on the spatial–temporal evolution and driving mechanism of urban land green use efficiency in the Yellow River Basin cities. *Ecol. Indic.* **2023**, *154*, 110672. [CrossRef]

74. Wu, H.; Fang, S.; Zhang, C.; Hu, S.; Nan, D.; Yang, Y. Exploring the impact of urban form on urban land use efficiency under low-carbon emission constraints: A case study in China's Yellow River Basin. *J. Environ. Manag.* **2022**, *311*, 114866. [[CrossRef](#)] [[PubMed](#)]
75. Zhou, S.; Liu, D.; Zhu, M.; Tang, W.; Chi, Q.; Ye, S.; Xu, S.; Cui, Y. Temporal and Spatial Variation of Land Surface Temperature and Its Driving Factors in Zhengzhou City in China from 2005 to 2020. *Remote Sens.* **2022**, *14*, 4281. [[CrossRef](#)]
76. Yang, Y.; Song, F.; Ma, J.; Wei, Z.; Song, L.; Cao, W. Spatial and temporal variation of heat islands in the main urban area of Zhengzhou under the two-way influence of urbanization and urban forestry. *PLoS ONE* **2022**, *17*, e0272626. [[CrossRef](#)] [[PubMed](#)]
77. Guoyi, L.; Liu, J.; Shao, W. Urban flood risk assessment under rapid urbanization in Zhengzhou City, China. *Reg. Sustain.* **2023**, *4*, 332–348. [[CrossRef](#)]
78. Zheng, L.; Wang, Y.; Li, J. Quantifying the spatial impact of landscape fragmentation on habitat quality: A multi-temporal dimensional comparison between the Yangtze River Economic Belt and Yellow River Basin of China. *Land Use Policy* **2023**, *125*, 106463. [[CrossRef](#)]
79. Dong, X.; Li, X.; Ye, Y.; Su, D.; Yang, R.; Lausch, A. Measuring urban thermal environment from accessibility-based perspective: A case study in a populous city. *Geogr. Sustain.* **2024**, *5*, 329–342. [[CrossRef](#)]
80. Ren, Z.; Tian, Z.; Wei, H.; Liu, Y.; Yu, Y. Spatiotemporal evolution and driving mechanisms of vegetation in the Yellow River Basin, China during 2000–2020. *Ecol. Indic.* **2022**, *138*, 108832. [[CrossRef](#)]
81. Leal, P.H.; Marques, A.C. The evolution of the environmental Kuznets curve hypothesis assessment: A literature review under a critical analysis perspective. *Heliyon* **2022**, *8*, e11521. [[CrossRef](#)] [[PubMed](#)]
82. Chen, Z.; Lin, J.; Huang, J. Linking ecosystem service flow to water-related ecological security pattern: A methodological approach applied to a coastal province of China. *J. Environ. Manag.* **2023**, *345*, 118725. [[CrossRef](#)] [[PubMed](#)]
83. Su, D.; Cao, Y.; Dong, X.; Wu, Q.; Fang, X.; Cao, Y. Evaluation of ecosystem services budget based on ecosystem services flow: A case study of Hangzhou Bay area. *Appl. Geogr.* **2024**, *162*, 103150. [[CrossRef](#)]
84. Gillner, S.; Vogt, J.; Tharang, A.; Dettmann, S.; Roloff, A. Role of street trees in mitigating effects of heat and drought at highly sealed urban sites. *Landsc. Urban Plan.* **2015**, *143*, 33–42. [[CrossRef](#)]
85. Yazdi, J. Optimal Operation of Urban Storm Detention Ponds for Flood Management. *Water Resour. Manag.* **2019**, *33*, 2109–2121. [[CrossRef](#)]

Disclaimer/Publisher's Note: The statements, opinions and data contained in all publications are solely those of the individual author(s) and contributor(s) and not of MDPI and/or the editor(s). MDPI and/or the editor(s) disclaim responsibility for any injury to people or property resulting from any ideas, methods, instructions or products referred to in the content.